Image and Vision Computing 29 (2011) 546–556

Contents lists available at ScienceDirect

Image and Vision Computing

journal homepage: www.elsevier.com/locate/imavis

SEDMI: Saliency based edge detection in multispectral images ☆

Cuong V. Dinh [a,c,*], Raimund Leitner [c], Pavel Paclik [b], Marco Loog [a], Robert P.W. Duin [a]

[a] Pattern Recognition Laboratory, Delft University of Technology, Delft, The Netherlands
[b] PR Sys Design, Delft, The Netherlands
[c] Carinthian Tech Research AG, Villach, Austria

ARTICLE INFO

Article history:
Received 29 June 2010
Received in revised form 23 May 2011
Accepted 3 June 2011

Keywords:
Multispectral image analysis
Edge detection
Saliency
Ensemble clustering

ABSTRACT

Detecting edges in multispectral images is difficult because different spectral bands may contain different edges. Existing approaches calculate the edge strength of a pixel locally, based on the variation in intensity between this pixel and its neighbors. Thus, they often fail to detect the edges of objects embedded in background clutter or objects which appear in only some of the bands.

We propose SEDMI, a method that aims to overcome this problem by considering the salient properties of edges in an image. Based on the observation that edges are rare events in the image, we recast the problem of edge detection into the problem of detecting events that have a small probability in a newly defined feature space. The feature space is constructed by the spatial gradient magnitude in all spectral channels. As edges are often confined to small, isolated clusters in this feature space, the edge strength of a pixel, or the confidence value that this pixel is an event with a small probability, can be calculated based on the size of the cluster to which it belongs.

Experimental results on a number of multispectral data sets and a comparison with other methods demonstrate the robustness of the proposed method in detecting objects embedded in background clutter or appearing only in a few bands.

1. Introduction

Edge detection for gray-scale images has been thoroughly studied and is well established. However, for color images and especially for multispectral images, this topic is still in its infancy and even defining edges for these images is a challenge [1]. There are two main approaches to detect edges in multi-channel images based on either monochromatic [2,3] or vector techniques [4–6]. The monochromatic approaches apply a gray-scale edge detection to each band and then combine the results over all the bands. Several combination rules have been used, e.g. the summation rule [3], the maximum rule [7], and the OR operation [8]. A more sophisticated combination technique is to fuse the individual responses using different weights [9].

Vector based approaches consider each pixel in a multispectral image as a vector in the spectral domain, then perform edge detection in this domain. These approaches can be further divided into two categories: multidimensional gradient [4,10,11] and vector order statistic [5,6,12]. The multidimensional gradient approach extends the gray-scale definition of gradient magnitude and direction to multispectral images. Di Zenzo [4] defines the gradient direction at a pixel as the direction in which its vector in the spectral domain has the maximum rate of change. Hence, an eigenvalue decomposition is applied to the set of partial derivatives at a pixel to determine the largest eigenvalue and its corresponding eigenvector. The largest eigenvalue is then considered as the edge magnitude and the eigenvector as the edge direction of this pixel. The disadvantage of this method is its sensitivity to texture because the gradient-based operators are sensitive to small change in intensity.

The vector order statistic approach follows the use of morphological operators for edge detection in gray-scale images [13], which calculates gradients as the difference between a dilation and an erosion. Trahanias et al. [5] order the pixels within a small window by the aggregate distances of each pixel to the others. Then, the edge strength of the pixel located at the center of the window is calculated as the deviation between the vector with the highest rank and the median vector. Evans and Liu [6] improve this method by defining the edge strength of a pixel as the maximum distance between any two pixels in its surrounding window. This helps to localize edge locations more precisely.

In the approaches discussed above, the edge strength of each pixel is computed locally based on the variations in the intensities of the pixels within a small, surrounding window. Consequently, besides extracting meaningful and useful edges, these approaches also extract many other spurious edges that arise from noise and background clutter [14,15]. For gray scale images, a common method to overcome this problem is based on the salient characteristic of edges in images [14,16]. This stems from visual attention theory that structurally salient features such as edges,

☆ This paper has been recommended for acceptance by Sinisa Todorovic.

* Corresponding author at: Pattern Recognition Laboratory, Delft University of Technology, Delft, The Netherlands. Tel.: +31 (0)15 27 88433.
E-mail address: v.c.dinh@tudelft.nl (C.V. Dinh).

0262-8856/$ – see front matter © 2011 Elsevier B.V. All rights reserved.
doi:10.1016/j.imavis.2011.06.002

blobs, and circles are pre-attentively distinctive. They attract our attention without the need to scan the entire image in a systematic manner [17]. The saliency of an edge can be defined as its stability of occurrence over scales [18] or the maximum over scales of normalized derivatives [19]. Saliency, according to information theory, is also related to the frequency or the probability of occurrence, i.e. events that occur rarely are more informative [20,21].

Motivated from these approaches, we recast the edge detection problem in multispectral images into detecting events that occur with a small probability in a newly defined feature space. The feature space is constructed by spatial gradient magnitudes of all pixels over all spectral bands (thereafter referred to as gradient magnitude feature space). We then introduce a saliency based edge detection in multispectral images (SEDMI) to detect such events.

The prominent characteristic of the gradient magnitude feature space is that edge pixels often fall in small, isolated clusters. The saliency (or the edge strength) of a pixel is then defined as the confidence value that this pixel belongs to a small cluster and subsequently, can be calculated based on the size of the cluster containing the pixel. As the constructed gradient magnitude feature space utilizes the global, structural image information, SEDMI recovers edges of objects surrounded by background clutter or objects appearing in a few bands of a multispectral image.

The rest of the paper is organized as follows. Section 2 provides additional motivation for SEDMI and discusses related work. Section 3 presents the SEDMI method. To demonstrate the effectiveness of our method, experimental results and a comparison with other methods are presented in Section 4. Sections 5 and 6 discuss related issues and draw conclusions.

2. Motivation and related work

2.1. Edge detection as detecting salient features

Salient features are image features assumed to be able to capture the most prominent structures in an image [21]. They may provide crucial clues for image analyses such as image matching and object detection. Salient features are often defined as the local extrema of some functions in the image. Thus, corners, junctions, blobs, and edges (local maxima of gradient magnitudes) can be considered as salient features [22].

According to information theory, saliency is related to the frequency of appearance: events that occur rarely are more informative [20,21]. Thus, salient features correspond to the events with small probabilities in a feature space defined by, for example, differential invariant features of the pixels over a range of scales [23]. Salient features can then be detected by applying a novelty detection technique to the constructed feature space [24]. Inspired by this approach, we recast the edge detection problem in multispectral images into detecting events with small probability (thereafter referred to as small probability events) in the feature space composed of the gradient magnitudes of the pixels in all channels.

The main assumption made in our method is that edges in a multispectral image are rare events. This assumption is reasonable because the frequency of occurrence of edges in an image is typically small ($O(m)$ in an $m \times m$ image). In addition, spectral differences on edges between objects are often systematic. This yields a similarity in the gradient magnitudes between these edge pixels. Therefore, they form a small, isolated cluster in the gradient magnitude feature space.

2.2. Towards clustering-based edge detection

As discussed earlier, the prominent characteristic of the gradient magnitude feature space is that edge pixels often fall in small, isolated clusters. Therefore, the cluster based novelty detection approach, which is based on the size of the cluster, is suitable for detecting edge pixels in the gradient magnitude feature space [25,26]. The smaller the cluster size corresponding to a pixel, the more likely this pixel is a small probability event. The cluster size of a pixel p can be defined as either the number of pixels in the cluster containing it [26] or the number of pixels within a hyper-sphere centered at p with radius w. w is determined by learning from a training set [25]. In our method, we use the former definition.

It should be noted that clustering methods often require prior knowledge about the data, such as the number of clusters and cluster shapes. For edge detection, however, such *a prior* knowledge is typically unavailable. To overcome this obstacle, we use ensemble clustering that is well known for its stability and robustness without any prior knowledge [27,28].

2.3. Related work on ensemble clustering

The main aim of data clustering is to partition an unlabeled data set into homogenous regions. However, it is an ill-posed problem due to the lack of prior information about the underlying data distribution [27,28]. By utilizing the fact that different clusterings (difference in algorithms or in the setting of each algorithm) applied to the same data set are able to capture different structures in the data, ensemble clustering has been shown to be a powerful method for improving the cluster result in terms of both robustness and stability.

In [28], a set of clustering results is transformed into a hyper-graph representation. In the hyper-graph, each vertex corresponds to a point in the data set and each hyper-edge, which can connect any set of vertices, represents a cluster in a clustering. Based on this representation, different consensus functions, e.g. Cluster-based Similarity Partitioning Algorithm (CSPA), HyperGraph Partitioning Algorithm (HGPA), and Meta-CLustering Algorithm (MCLA), can be used to produce the final clustering result.

In [27], an evidence accumulation clustering algorithm is proposed. In the algorithm, the results of multiple clusterings are summarized into a Co-Association (CA) matrix, in which each element is the number of times a pair of points is assigned to the same cluster. Subsequently, the final clustering can be computed by applying a hierarchical clustering to the CA matrix. In fact, the CA matrix can be considered as a similarity measurement between points. The more frequently two points are in the same cluster, the more similar they are.

It should be noted that we use ensemble clustering in our method to estimate the cluster size corresponding to a pixel but not to generate the final clustering as in the above methods. As demonstrated in Section 3.4, the estimated cluster size of a pixel is equal to the sum of the co-association values of this pixel with respect to all pixels in the multispectral images. This provides a strong connection between our method and the evidence accumulation clustering method.

3. SEDMI method

3.1. Constructing the feature space

For each channel of an n-channel multispectral image, we compute its gradient magnitude using a Gaussian derivative [29]. Each pixel is then represented by an n-component vector composed of the gradient magnitudes of this pixel over all channels. Thus, the gradient magnitude feature space contains M such vectors, where M is the number of pixels in the image.

3.2. Performing ensemble clustering

We perform ensemble clustering in the gradient magnitude feature space to estimate the cluster size for the pixels in the image. One important requirement in ensemble clustering is the diversity in the clustering results. This requirement is needed to ensure that

different clusterings preserve different structures in the image and do not yield identical data partitions. Therefore, we use a simple k-means as the base clustering algorithm. At each clustering, we randomly choose the number of clusters and the initial cluster centers.

After each clustering, we calculate for each pixel the size of the cluster containing it. The estimated (expected) cluster size of a pixel p_i, denoted as $EC(p_i)$, is then calculated as the mean (average) of the size of the clusters containing p_i generated by N clusterings:

$$EC(p_i) = \frac{\sum_{t=1}^{N} C_{i,t}}{N} \quad (1)$$

where $C_{i,t}$ is the size of the cluster containing pixel p_i at clustering t.

3.3. Calculating edge strength map

We calculate the edge strength of a pixel based on its cluster size estimated by the ensemble clustering. A pixel is an edge pixel or an event with small probability if it belongs to small clusters. Therefore, the smaller the expected cluster size of a pixel, the more probable this pixel is a small probability event. Thus, the confidence value that a pixel p_i is a small probability event, or the edge strength of p_i, denoted as $ES(p_i)$, can be calculated as follows:

$$ES(p_i) = 1 - \frac{EC(p_i)}{M}. \quad (2)$$

It should be noted that an image with high spatial resolution may cause a high computational cost because of the ensemble clustering procedure. In this case, we may reduce the computational cost by (i) randomly selecting a subset of pixels, (ii) performing the ensemble clustering on this subset to compute the edge strength for the pixels in this subset, and (iii) using a regression algorithm, e.g. knn-regression [30], to estimate the edge strength for the remaining pixels in the image.

3.4. Connection with the evidence accumulation clustering

Our algorithm to compute the cluster size for a pixel is strongly connected with the evidence accumulation clustering. We will show that the estimated cluster size of a pixel in our algorithm is equal to the sum of the co-association values between this pixel and all the pixels including itself. The following deduction demonstrates this claim. Denote $a_{ij,\,t}$ the association value between pixels p_i and pixel p_j at clustering t. $a_{ij,\,t}$ equals 1 if p_i and p_j are in the same cluster and 0 otherwise. Note that $a_{ii,\,t} = 1$. From Eq. (1), the estimated cluster size of p_i is:

$$EC(p_i) = \frac{\sum_{t=1}^{N} C_{i,t}}{N} = \frac{\sum_{t=1}^{N}\sum_{j=1}^{M} a_{ij,t}}{N} = \sum_{j=1}^{M} \frac{\sum_{t=1}^{N} a_{ij,t}}{N}. \quad (3)$$

Denote $CA(i, j)$ the co-association value between pixels p_i and p_j after N clusterings. $CA(i, j)$ is the number of times the two pixels being assigned to the same cluster normalized by N. Then Eq. (3) becomes:

$$EC(p_i) = \sum_{j=1}^{M} CA(i,j). \quad (4)$$

Table 1
Co-association between a pixel p_i and all the pixels in the feature space.

	p_1	p_2	⋯	p_M	Sum (cluster size)
Clustering 1	$a_{i1,1}$	$a_{i2,1}$	⋯	$a_{iM,1}$	$C_{i,1}$
Clustering 2	$a_{i1,2}$	$a_{i2,2}$	⋯	$a_{iM,2}$	$C_{i,2}$
⋮	⋮	⋮		⋮	⋮
Clustering N	$a_{i1,N}$	$a_{i2,N}$	⋯	$a_{iM,N}$	$C_{i,N}$
Sum	$N\times CA(i,1)$	$N\times CA(i,2)$	⋯	$N\times CA(i,M)$	$N\times EC(p_i)$

Table 2
Properties of the four data sets used in experiments.

Data sets	No. channels	Spatial resolution
AI I	20	100×100
AI II	20	100×100
SEM/EDX	8	128×128
Scene	31	820×820

A graphical illustration of our claim is shown in Table 1. The sum across a row t ($t = 1 \cdots N$) corresponds to the size of the cluster containing the pixel under consideration (p_i) at clustering t; while the sum across a column j ($j = 1 \cdots M$) is equal to the co-association value between the pixels p_i and p_j times N. It is obvious that the sum across all rows equals to the sum across all columns in a matrix. Thus, Eq. (4) is deduced.

On the other hand, the co-association of two pixels represents the similarity, or the inverse distance, between them. From this point of view, the way a pixel is considered as a small probability event in our method is confirmed by the R-ordering in statistics [31]. The greater the distance between a point of interest and all other points in the feature space, the more likely this point is an event that has small probability.

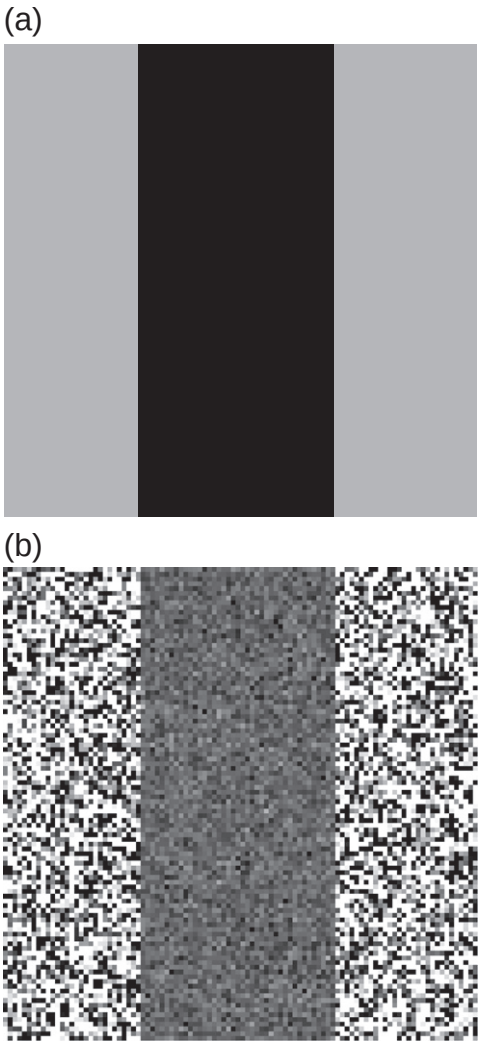

Fig. 1. A channel in the AI I data set. (a) The content of the synthetic image without noise (object is located in the middle) and (b) a corrupted image with the SNRs of 16 dB in the object region and 0.2 dB in the background region. Dark color means high intensity.

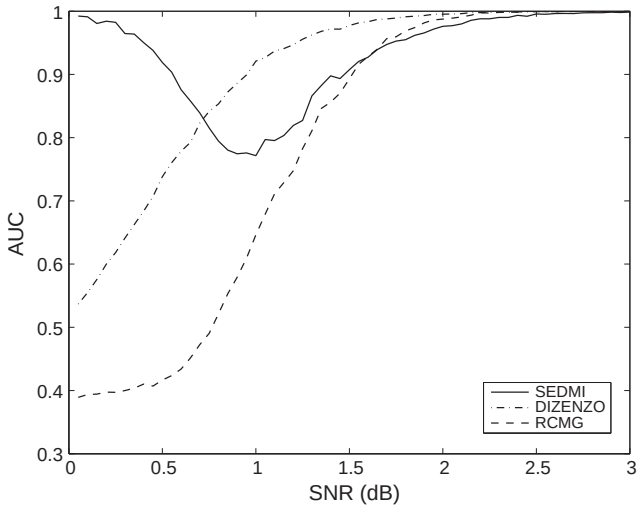

Fig. 2. AUC curves produced by SEDMI (solid line), Di Zenzo's method (dot dashed line), and the RCMG method (dashed line) for the AI I data set. The horizontal axis shows the SNR with respect to the background noise level.

It should be noted that although the estimated cluster size of a pixel can be calculated from the co-association matrix, we do not need to generate the co-association matrix explicitly. Thus, it avoids the problem of quadratic memory required to store the $M \times M$ matrix for large M in the evidence accumulation clustering algorithm.

4. Experimental results

We compare the edge detection results between the SEDMI and two other methods: the Di Zenzo method [4] and the Robust Color Morphological Gradient (RCMG) method proposed by Evans and Liu [6]. We select these two methods for comparison as they represent two main approaches for edge detection in multispectral images: multidimensional gradient and vector order statistics, respectively.

For the RCMG method [6], the mask size is set to 5×5 and the number of rejected vector pairs is set to 8 as recommended by the authors. For the SEDMI method, the gradient magnitude for each pixel is computed by a Gaussian derivative with $\sigma = 1$. In the ensemble clustering, the number of clusterings is set to 200. At each clustering, the cluster centers are randomly selected and the number of clusters varies from 3 to 15. We use this configuration for all of the studied multispectral data sets.

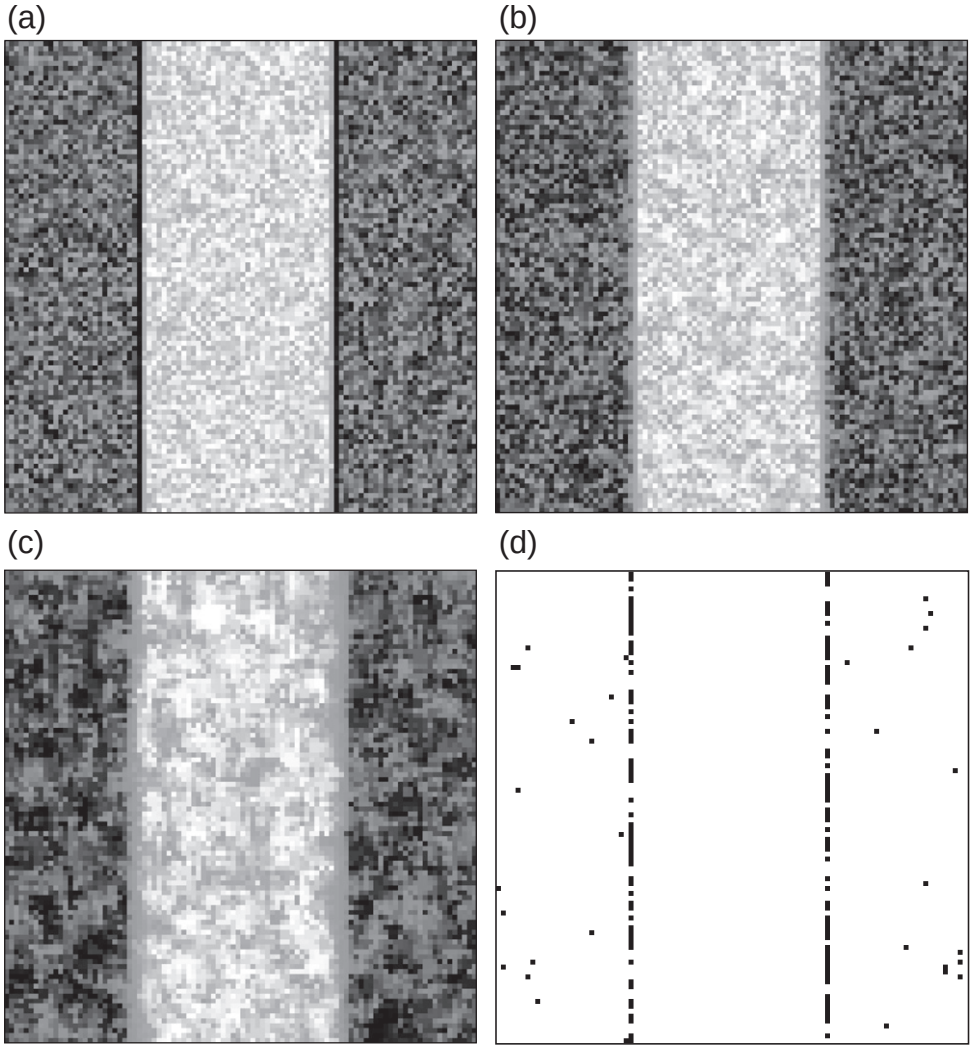

Fig. 3. Edge strength maps generated by (a) SEDMI (0.98), (b) Di Zenzo's method (0.59), and (c) the RCMG method (0.39) for the AI I data set with the background noise level corresponding to a SNR of 0.2 dB. Dark color means high edge strength. The corresponding AUC values are shown in brackets. Figure (d) shows the best binary edge map generated by the SEDMI method.

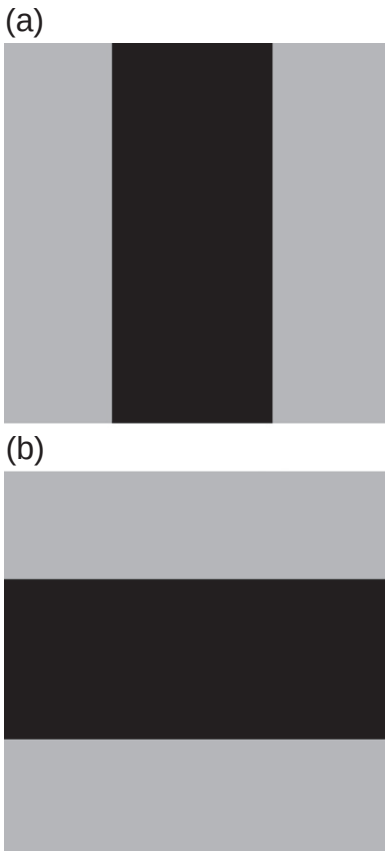

Fig. 4. Two representative channels in the AI II data set. (a) A channel with the vertical bar object and (b) a channel with the horizontal bar object.

Four multispectral data sets are used for the evaluation: two artificial images (AI I and AI II) and two from real world applications (SEM/EDX and Scene). The properties of these data sets are shown in Table 2.

We evaluate edge detection results in term of both quantitative and subjective measurements. For the quantitative measurement, we use the area under the ROC curves (AUC) criteria following [32,33]. The receiver operating characteristic (ROC) curve [34] is a plot of the true positive edge rate against the false positive edge rate with regards to different thresholds.

For each multispectral data set, we first apply the three methods to generate the corresponding edge strength maps. We then put these edge strength maps into the same thinning process introduced in [35]. In this process, a pixel is only considered as an edge if its edge strength is a local maximum in the horizontal or vertical direction. Finally, we generate the binary edge maps by thresholding the corresponding edge strength maps.

Using the ROC curve, the best threshold is typically determined at the point which yields the minimum sum of false positive and false negative rates [36]. For edge detection problems, however, this threshold often results in many false positive edge pixels because the

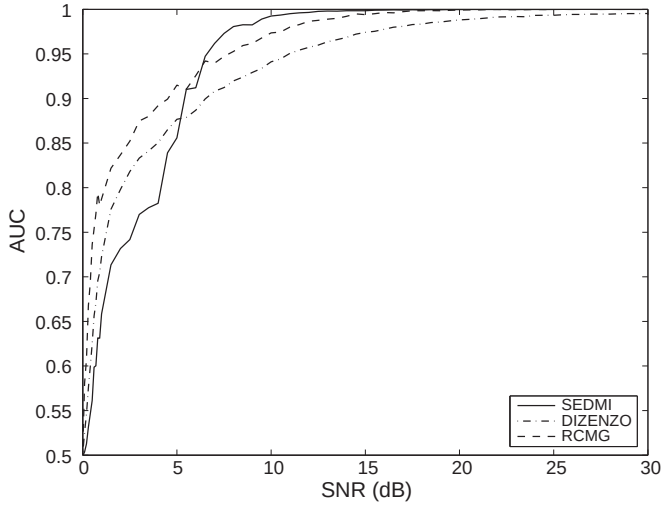

Fig. 5. AUC curves for the AI II data set generated by SEDMI (solid line), Di Zenzo's method (dot dashed line), and the RCMG method (dashed line). The horizontal axis shows the SNR with respect to the noise level added to the data set.

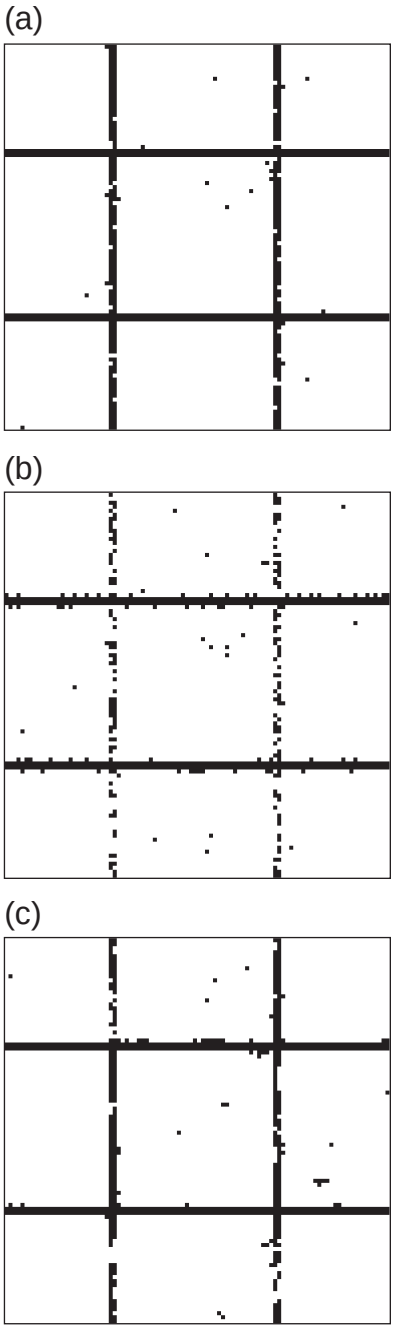

Fig. 6. The best binary edge maps generated for the AI II data set with the SNR of 16 dB by (a) the SEDMI method (0.998), (b) Di Zenzo's method (0.972), and (c) the RCMG method (0.993). The corresponding AUC values are shown in brackets.

number of background pixels is normally substantially larger than that of edge pixels (e.g. 9800 background pixels versus 200 edge pixels in the AI I data set). Therefore, we select the threshold that yields the minimum total number of false positive and false negative edge pixels for the artificial data. For the real data, we select the threshold at which a best subjective result is obtained.

4.1. Artificial data

4.1.1. Objects surrounded by background clutter

Using the AI I data set, we investigate the behavior of the three edge detection methods when the objects in an image are embedded by severe noise or background clutter. We generated a multispectral image composed of 20 channels. We used the same binary image of size 100×100 with intensity of 0.7 in the object region and 0.3 in the background region for each channel. The content of the synthetic image without noise is shown in Fig. 1a. The object is located in the middle from column 30 to column 70. Thus, edge pixels are located at columns 30 and 70. A fixed, low Gaussian noise level corresponding to a signal to noise ratio (SNR) of 16 dB is added to the object region. The noise level in the background region varies with the corresponding SNRs from 0 to 3 dB. Fig. 1b shows an example of a channel for a SNR of 0.2 dB with respect to the background noise level.

Fig. 2 depicts the AUC curves produced by (a) SEDMI (solid line), (b) the Di Zenzo method (dot dashed line), and (c) the RCMG method (dashed line). The horizontal axis shows the SNR with respect to the noise level in the background region. The vertical axis displays the AUC value. SEDMI outperforms Di Zenzo's method and the RCMG method for low SNRs (from 0 to 0.75 dB) or high noise levels. As SNR exceeds 0.75 dB, the Di Zenzo method produces the largest AUC value. SEDMI continues performing better than the RCMG method as SNR grows to 1.65 dB. For SNRs between 1.65 dB and 2.5 dB, the other two methods work slightly better than SEDMI.

SEDMI is markedly more robust to severe noise in the background region (background clutter) than the other methods. For high background noise levels (the corresponding SNRs around 0.01 dB), SEDMI yields an AUC value of approximately 1 while the AUC values produced by the Di Zenzo and the RCMG methods are both smaller than 0.6. In this case, the difference in gradient magnitude between the edge pixels is substantially smaller than that between an edge pixel and a pixel in the background region. This leads to the formation of edge pixels as a small, isolated cluster in the global gradient magnitude feature space. Thus, SEDMI detects these edge pixels. Di Zenzo's and the RCMG methods are greatly inferior to SEDMI in dealing with such severe background noise because they do not use the global statistical information in the spatial domain of the image. The edge strength of a pixel is calculated based on a local window. In the background region, a combination between a noisy pixel and its neighbors whose differences in intensities are large leads to a large gradient magnitude for this noisy pixel, even larger than the gradient magnitudes of the true edge pixels. Subsequently, these methods incorrectly determine this noisy pixel as an edge pixel.

The AUC produced by SEDMI decreases to a minimum value of 0.76 as the SNR increases to around 1.0 dB, and then increases again to 1. For small SNRs, only a small number of pixels in the background exhibit similar intensities with those of pixels in the object region. When the SNRs increase, the number of background and object pixels having similar intensities increases too, and thus more background and edge

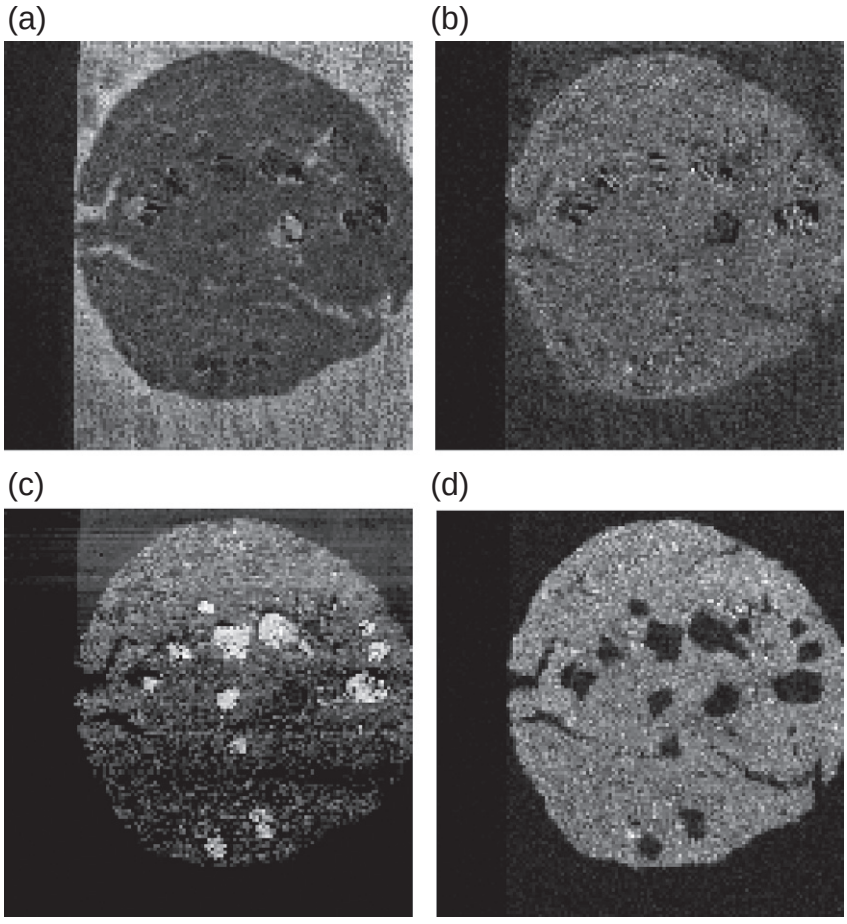

Fig. 7. Four channels in the SEM/EDX dataset. (a) The second channel, (b) the fourth channel, (c) the sixth channel, and (d) the eighth channel.

pixels exhibit similar gradient magnitudes. They are then grouped into the same clusters. This makes it difficult for SEDMI to estimate the cluster size for these edge pixels correctly.

The robustness to background clutter of the SEDMI method is further illustrated by the edge strength map and the binary edge map in Fig. 3. Fig. 3a–c shows the gradient maps generated by (a) SEDMI, (b) the Di Zenzo method, and (c) the RCMG method for a SNR of 0.2 dB. The darker a pixel in the edge strength map, the higher the edge strength in that location. Most of the true edge pixels dominate the highest edge strength values in the edge strength map produced by SEDMI (the

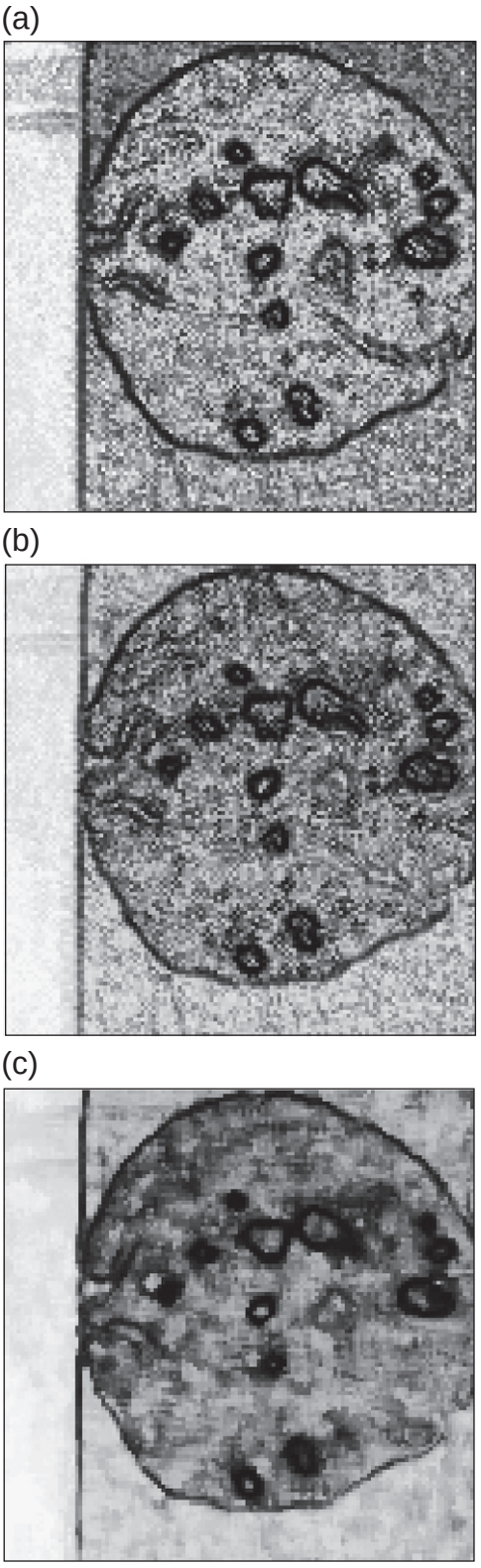

Fig. 8. Edge strength maps generated on the SEM/EDX dataset by (a) SEDMI, (b) Di Zenzo's method, and (c) the RCMG method. Dark color means high edge strength.

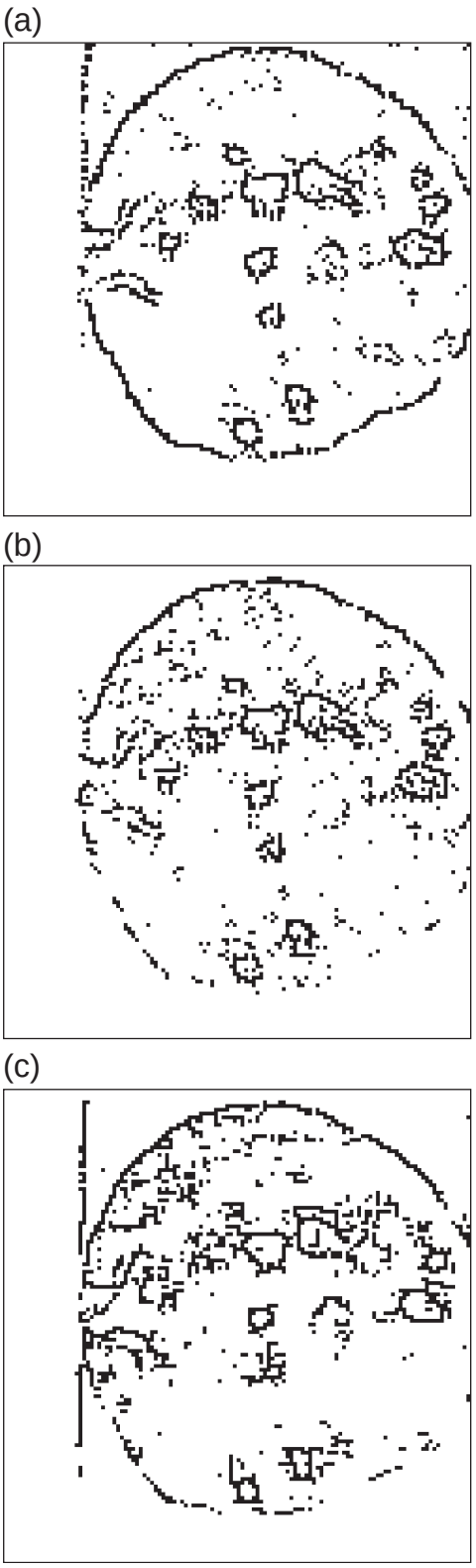

Fig. 9. The best subjective binary edge maps generated for the SEM/EDX dataset by (a) SEDMI, (b) Di Zenzo's method, and (c) the RCMG method.

corresponding AUC is 0.98). As a result, these edge pixels are correctly selected when thresholding the gradient map. The best binary edge map created by SEDMI using the minimum total number of false positive and false negative edge pixels criterion is depicted in Fig. 3d.

In contrast, Di Zenzo's and the RCMG methods calculate substantially smaller edge strengths for the true edge pixels than for the noisy pixels in the background region (the corresponding AUCs are 0.59 and 0.39, respectively). These noisy pixels then dominate the binary edge map. Consequently, the best binary edge maps generated according to the above criterion assign all pixels to background. We note that if the threshold is determined by the point in the ROC curve that gives the minimum sum of false positive and false negative rates, then most of the noisy pixels are classified as edge pixels by these two methods.

4.1.2. Objects occurring in a few bands

The AI II data set contains objects appearing in a few spectral bands. There are two objects of interest a vertical bar and a horizontal bar. The objects have the same intensity values in the images. The vertical bar appears in the first two bands whilst the horizontal bar appears in the remaining eighteen bands. The contents of the synthetic images without noise containing the vertical and the horizontal objects are shown in Fig. 4a–b. All of the bands in the data set are then corrupted by the independent Gaussian noise. It should be noted that applying a thinning process to this data set will generate offset edges because in the case of binary image corrupted by noise, edge strengths at two sides of the

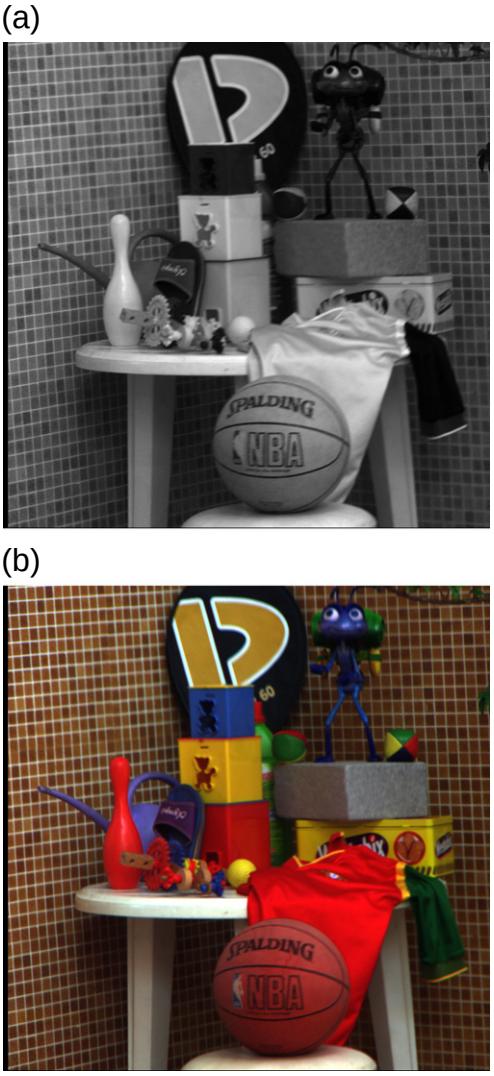

Fig. 10. The scene data set. (a) A gray scale image (channel 28) and (b) the reconstructed color image of the data set (channels 28, 14, and 4 are used, respectively, as the red, green, and blue channels for the reconstruction).

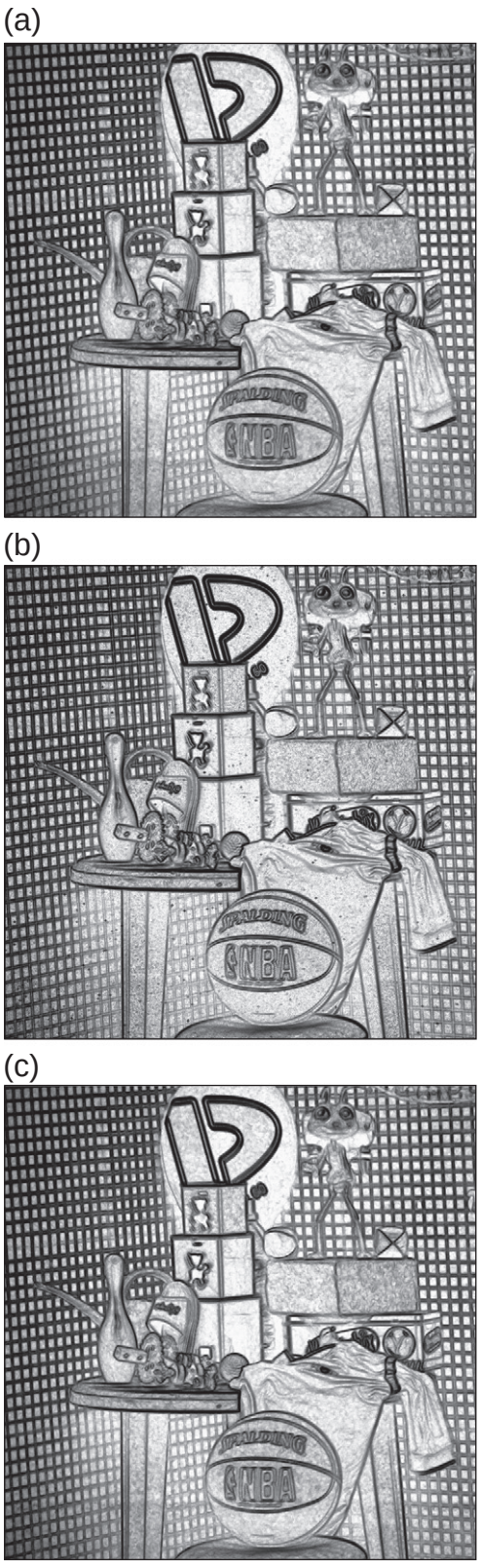

Fig. 11. Edge strength maps generated on the scene dataset by (a) SEDMI, (b) Di Zenzo's method, and (c) the RCMG method. Dark color means high edge strength.

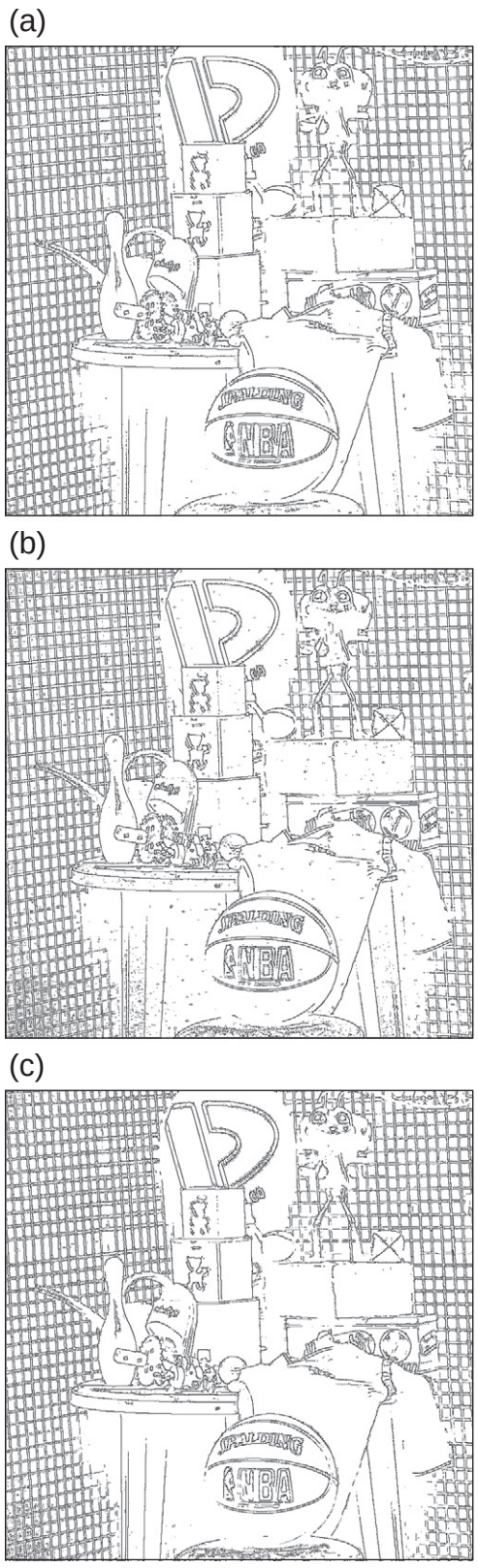

Fig. 12. The best subjective binary edge maps generated for the scene dataset by (a) SEDMI, (b) Di Zenzo's method, and (c) the RCMG method.

edges differ from each other only due to noise. Therefore, for all methods, we exclude the thinning process from this experiment.

Fig. 5 shows the AUC curves produced by the three methods with respect to various levels of Gaussian noise. For SNR lower than 6.0 dB, the RCMG method outperforms both the Di Zenzo method and SEDMI. As SNR exceeds 6.0 dB, SEDMI performs better than the other two methods.

Fig. 6 shows the best binary edge maps generated by (a) SEDMI, (b) the Di Zenzo method, and (c) the RCMG for the SNR of 16 dB. The corresponding AUCs are 0.998, 0.972 and 0.993, respectively. All three methods detect the horizontal bar well as it appears in most of the bands (18/20). The Di Zenzo method detects many noisy pixels close to the horizontal bar while the vertical bar exhibits discontinuous edges. Compared with SEDMI, the RCMG method misses more edge pixels for the vertical bar as reflected by a slightly lower AUC value.

4.2. Real world data sets

4.2.1. SEM/EDX data set

This data set is a collection of scans of detergent powder obtained from a scanning electron microscopy using energy-dispersive X-ray microanalysis (SEM/EDX). The data consists of eight 128×128 images that correspond to particular chemical substances. [37]. The data set is noisy in both spatial and spectral domains. Four representative channels are shown in Fig. **7**a–d. The crucial task is to reveal the spatial arrangement of three clusters: the solid, the active, and the porous regions of the detergent powder.

Fig. 8a–c shows the edge strength maps generated for this data set by the evaluated methods. SEDMI exhibits a high contrast between the edge and the background/noisy pixels. Thus, the method distinguishes edge pixels from noise pixels in the image.

Fig. 9a–c shows the best subjective binary edge results generated by (a) the SEDMI method, (b) the Di Zenzo method, and (c) the RCMG method (binary edge maps based on various thresholds are provided in the Supplement, Figures S1–2). The figures demonstrate that the SEDMI method is less affected by noise than the other two methods. SEDMI detects edges along the boundaries between the active and the porosity (particularly in the lower part of the image) whilst the other methods suffer heavily from the noise and fail.

In terms of continuity, edges generated by the RCMG method are more continuous than those generated by the SEDMI and the Di Zenzo methods, e.g. the vertical line on the left side of the image. It is because in the RCMG method, neighbor pixels tend to have similar gradient magnitude values. On the other hand, however, this similarity may result in spurious edges in the noisy region, e.g. the region under the upper curve in the image.

4.2.2. Scene data set

Foster's group created a database containing 30 hyperspectral images of natural scenes [38]. Eight representative scenes are available from [39]. We select the fifth scene for our experiment because of two reasons. Firstly, it contains many man-made objects. Therefore, we know exactly their boundary, i.e. we know where edges should be. Secondly, these objects are surrounded by a heavily textured wall. Fig. 10 shows (a) a gray scale image (channel 28) and (b) the reconstructed color image of the data. Channels 28, 14, and 4 are used, respectively, as the red, green, and blue channels for the reconstruction.

The data set under consideration contains 31 channels with a large spatial resolution of 820×820 pixels. As discussed in Section 3.3, we reduce the computational cost by computing the edge strength values for 5000 randomly selected pixels and then estimating the edge strength values for the remaining pixels using a k-NN regression. The number of nearest neighbors used in the k-NN regression is set to 50.

Edge strength maps generated by the three methods are shown in Fig. 11a–c. Fig. 12a–c shows the best subjective binary edge results by thresholding the three edge strength maps (binary edge maps generated using various thresholds can be found in the Supplement, Figures S3–4). The SEDMI method is able to locate edges of most of the

objects such as the text on the ball and the toys on the left side of the table. However, the method does not detect as many edges of the textured wall on the bottom right as the RCMG method does. On the other hand, the Di Zenzo and the RCMG methods generate many spurious edges on the chair and under the ball due to the variance in intensity of the chair's surface. As demonstrated by the AI I data set, SEDMI is better in dealing with such a variance by using the assumption that edges are rare events in the image. Pixels appearing with higher frequency manifest smaller edge strength values; hence, these pixels are not classified as edges.

5. Discussion

The main advantage of the SEDMI method is the ability to deal with images in which objects are surrounded by severe noise and background clutter. Typical edge detection techniques such as the Di Zenzo method [4] and the RCMG method [6] compute edge strength of a pixel by considering its small, surrounding window. This results in misclassifying the noisy pixels as edge pixels in such a circumstance because the noisy pixels in noisy images may have significantly different intensities compared with their neighbors. Our approach overcomes this problem (c.f. Sections 4.1.1 and 4.2) by calculating the edge strength of a pixel based on its sparseness in the global gradient magnitude feature space. As a result, edge strengths of noisy pixels, which appear in the image with high frequency, are smaller than those of the edge pixels.

In hyperspectral images, objects appearing in one band may be absent in other bands. Moreover, a broad spectral band might dominate other bands which are more narrow in the spectral domain. Therefore, detecting objects which appear in such narrow spectral bands becomes difficult. As defined by our approach, edge pixels appearing in a few bands exhibit high similarity to one another. These pixels then form a small cluster in the feature space and hence, are detected by SEDMI.

We note that if severe noise (corresponding to low SNRs) is distributed independently in an image where objects appear in all bands, e.g. the AI I data set, Di Zenzo's method and SEDMI perform similarly and both are inferior to the RCMG method. The performance of the RCMG method results from its novel use of the pairwise pixel rejection scheme in calculating the variance in intensities of pixels within a small window. In such a case, applying a smoothing process before using SEDMI will substantially improve the edge detection result.

In terms of complexity, all the three methods are linearly dependent on the number of pixels in the image. SEDMI requires more computation than the other two methods due to the use of the ensemble clustering process. Ensemble clustering requires $O(M\times C\times N)$, where M is the number of pixels in the image; C is the number of clusters in each clustering and N is the number of times doing the clustering. The clustering process can be speeded up by i) performing ensemble clustering on a subset of pixels, which then requires $O(K\times C\times N)$ where K is the number of pixels in the subset; and then ii) generating edge strength map of the whole image using knn-regression algorithm, which requires $O(M\times log(K))$ in average [40]. It should also be noted that the use of the ensemble clustering in our method is to detect events with small probability in the feature space. We are, however, not restricted to using this type of clustering. Other techniques such as the density based technique can also be employed.

In this paper we focus on estimating edge strength for every pixel in the image. We note, however, that more sophisticated thinning approaches than the technique used [35] can be applied to multispectral edge detectors that provide accurate edge direction. Therefore, estimating the gradient direction of a pixel is an interesting continuation of the current research.

6. Conclusions

We have presented a saliency based approach for edge detection in multispectral images. First, we constructed the gradient magnitude feature space which contains spatial gradient magnitudes in all spectral channels. This feature space is composed of global information in both spatial and spectral domains. The key characteristic of this feature space w.r.t. the edge detection problem is that edges often stay in small, isolated clusters. Second, based on the assumption that edges are rare events in an image, we recast the edge detection problem into detecting events with small probability in the feature space. This assumption is reasonable as the proportion of edge pixels in an image is generally small.

Using the key characteristic of the feature space, we then estimated the confidence value that a pixel is a small probability event based on the size of the cluster containing it. The estimation is reliably produced by ensemble clustering. The confidence value is then interpreted as the edge strength of the pixel. Thus, the smaller the cluster size corresponding to a pixel, the more probable it is this pixel does belong to an edge in the image.

Experimental results on a number of multispectral data sets show that the proposed method gives promising results, especially in detecting objects embedded in background clutter or appearing in a few bands. The results also confirm that the rarity is an important property of edges in images and this property should be studied further. It also holds for other salient features in an image such as corners, junctions, and blobs. To construct suitable feature space to detect these features in a hyperspectral images may be interesting topics for future research.

Acknowledgements

The authors would like to thank Sergey Verzakov, David Tax and Yan Li for useful discussions. We thank the anonymous reviewers for fruitful comments and stimulating questions which greatly improved the revised manuscript. This research is supported by Carinthian Tech Research AG, Austria through the Austrian COMET funding program.

Appendix A. Supplementary data

Supplementary data to this article can be found online at doi:10.1016/j.imavis.2011.06.002.

References

[1] A. Koschan, M. Abidi, Detection and classification of edges in color images, Signal Processing Magazine, Special Issue on Color Image Processing 22 (2005) 64–73.
[2] G. Robinson, Color edge detection, Optical Engineering 16 (1977) 479–484.
[3] M. Hedley, H. Yan, Segmentation of color images using spatial and color space information, Journal of Electronic Imaging 1 (1992) 374–380.
[4] S.D. Zenzo, A note on the gradient of a multi-image, Computer Vision, Graphics, and Image Processing 33 (1986) 116–125.
[5] P. Trahanias, A. Venetsanopoulos, Color edge detection using vector order statistics, IEEE Transactions on Image Processing 2 (1993) 259–264.
[6] A.N. Evans, X.U. Liu, A morphological gradient approach to color edge detection, IEEE Transactions on Image Processing 15 (6) (2006) 1454–1463.
[7] T. Kanade, S. Shafer, Image understanding research at CMU, Proceedings of Image Understanding Workshop, 1987, pp. 32–40.
[8] J. Fan, D.K.Y. Yau, A.K. Elmagarmid, W.G. Aref, Automatic image segmentation by integrating color-edge extraction and seeded region growing, IEEE Transactions on Image Processing 10 (2001) 1454–1466.
[9] T. Carron, P. Lambert, Color edge detector using jointly hue, saturation and intensity, IEEE International Conference Image Processing, volume 3, 1994, pp. 977–981.
[10] A. Cumani, Edge detection in multispectral images, Graphical Models and Image Processing 53 (1) (1991) 40–51.
[11] M. Chapron, C. Ensea-Etis, A color edge detector based on statistical rupture tests, IEEE International Conference Image Processing, volume 2, 2000.
[12] P.J. Toivanen, J. Ansamäki, J.P.S. Parkkinen, J. Mielikäinen, Edge detection in multispectral images using the self-organizing map, Pattern Recognition Letters 24 (16) (2003) 2987–2994.

[13] R.M. Haralick, S.R. Sternberg, X. Zhuang, Image analysis using mathematical morphology, IEEE Transactions on Pattern Analysis and Machine Intelligence 9 (4) (1987) 532–550.
[14] P. Rosin, Edges: saliency measures and automatic thresholding, Geoscience and Remote Sensing Symposium, 1995. IGARSS'95.'Quantitative Remote Sensing for Science and Applications', International. Volume 1, 1995, pp. 93–95, vol. 1.
[15] G. Papari, N. Petkov, Adaptive pseudo dilation for gestalt edge grouping and contour detection, IEEE Transactions on Image Processing 17 (10) (2008) 1950–1962.
[16] A. Rosenfeld, R.A. Hummel, S.W. Zucker, Scene labeling by relaxation operations, IEEE Transactions on Systems, Man and Cybernetics 6 (6) (1976) 420–433.
[17] A. Sha'asua, S. Ullman, Structural saliency: the detection of globally salient structures using a locally connected network, Computer Vision., Second International Conference on, December 1988, pp. 321–327.
[18] D. Marr, E. Hildreth, Theory of edge detection, Proceedings of Royal Society of London, 1980, pp. 187–217.
[19] T. Lindeberg, Edge detection and ridge detection with automatic scale selection, Journal of Computer Vision 30 (November 1998) 117–156.
[20] J. van de Weijer, T. Gevers, A. Bagdanov, Boosting color saliency in image feature detection, IEEE Transactions on Pattern Analysis and Machine Intelligence 28 (1) (2006) 150–156.
[21] M. Loog, F. Lauze, The improbability of Harris interest points, IEEE Transactions on Pattern Analysis and Machine Intelligence 32 (2010) 1141–1147.
[22] Piater, J.H.: Visual feature learning. PhD thesis, Department of Computer Science, UMASS Amherst (2001).
[23] K.N. Walker, T.F. Cootes, C.J. Taylor, Locating salient object features, Proceedings of the British Machine Vision Conference, 1998, pp. 557–566.
[24] D. Lisin, E. Riseman, A. Hanson, Extracting salient image features for reliable matching using outlier detection techniques, Proceedings of the third international conference on Computer vision systems. Volume 2626, 2003, pp. 481–491.
[25] E. Eskin, A. Arnold, M. Prerau, L. Portnoy, S. Stolfo, A geometric framework for unsupervised anomaly detection, Applications of Data Mining in Computer Security, Kluwer Academic Publisher, 2002.
[26] Z. He, X. Xu, S. Deng, Discovering cluster-based local outliers, Pattern Recognition Letters 24 (9–10) (2003) 1641–1650.
[27] A.L.N. Fred, A.K. Jain, Combining multiple clusterings using evidence accumulation, IEEE Transactions on Pattern Analysis and Machine Intelligence 27 (6) (2005) 835–850.
[28] A. Strehl, J. Ghosh, Cluster ensembles—a knowledge reuse framework for combining multiple partitions, Journal of Machine Learning Research 3 (2003) 583–617.
[29] J. Canny, A computational approach to edge detection, IEEE Transactions on Pattern Analysis and Machine Intelligence (1986) 679–698.
[30] R.P.W. Duin, P. Juszczak, D.D. Ridder, P. Paclik, E. Pekalska, D.M.J. Tax, PRTools: A Matlab Toolbox for Pattern Recognition, http://www.prtools.org/.
[31] V. Barnett, The ordering of multivariate data, Journal of the Royal Statistical Society 139 (1976) 318–355.
[32] K. Bowyer, C. Kranenburg, S. Dougherty, Edge detector evaluation using empirical roc curves, Computer Vision and Image Understanding 84 (1) (2001) 77–103.
[33] S. Konishi, A.L. Yuille, J.M. Coughlan, S.C. Zhu, Statistical edge detection: learning and evaluating edge cues, IEEE Transactions on Pattern Analysis and Machine Intelligence 25 (1) (2003) 57–74.
[34] D. Green, J. Swets, Signal Detection Theory and Psycho-physics, Peninsula Publishing, 1988.
[35] J.S. Lim, Two Dimensional Signal and Image Processing, Addison-Wesley, 1990.
[36] W.J. Krzanowski, D.J. Hand, ROC Curves for Continuous Data, Chapman & Hall/CRC, 2009.
[37] P. Paclik, R.P.W. Duin, G.M.P. van Kempen, R. Kohlus, Segmentation of multi-spectral images using the combined classifier approach, Journal of Image and Vision Computing 21 (6) (2005) 473–482.
[38] S.M.C. Nascimento, F.P. Ferreira, D.H. Foster, Statistics of spatial cone–excitation ratios in natural scenes, Journal of the Optical Society of America A 19 (8) (2002) 1484–1490.
[39] D.H. Foster, The Hyperspectral Images of Natural Scenes Dataset, http://personalpages.manchester.ac.uk/staff/david.foster/2002.
[40] A.W. Moore, Efficient memory-based learning for robot control, Technical Report UCAM-CL-TR-209, University of Cambridge, Computer Laboratory, 1990.